EUROPEAN ORGANIZATION FOR NUCLEAR RESEARCH

29 October 2008

# 2008 Status Report of the HARP–CDP group

**The HARP–CDP group**

A. Bolshakova, I. Boyko, G. Chelkov, D. Dedovitch, A. Elagin, M. Gostkin, S. Grishin, A. Guskov, Z. Kroumchtein, Yu. Nefedov, K. Nikolaev, and A. Zhemchugov

**JINR, Dubna, Russian Federation**

F. Dydak* and J. Wotschack

**CERN, Geneva, Switzerland**

A. De Min

**Politecnico di Milano and INFN, Sezione di Milano-Bicocca, Milan, Italy**

V. Ammosov, V. Gapienko, V. Koreshev, A. Semak, Yu. Sviridov, E. Usenko, and V. Zaets

**IHEP, Protvino, Russian Federation**

CERN-SPSC-2008-027 / SPSC-SR-036
03/11/2008

*) Contactperson (*friedrich.dydak@cern.ch*)

CONTENTS

**1 Introduction** **3**

**2 Detector characteristics and performance** **3**

**3 Comparison of Geant4 hadron generators with data** **3**

3.1 Geant4 physics lists . . . . . 4

3.2 HARP–CDP physics list . . . . . 4

**4 Large-angle hadron production cross-sections** **6**

4.1 Inclusive cross-sections . . . . . 6

4.2 Comparison with E802 results . . . . . 10

4.3 Comparison with E910 results . . . . . 11

4.4 Comparison with results from ‘Official’ HARP . . . . . 11

4.5 Physics reach of HARP–CDP and of OH publications . . . . . 12

**5 LSND anomaly** **14**

5.1 HARP–CDP measurements versus LSND simulations . . . . . 15

**6 HARP–CDP publications and reports at conferences** **16**

**7 Prospects for further results from HARP–CDP** **16**

**8 Request to the SPSC** **16**

## 1 INTRODUCTION

Because of a deep split of opinion over physics analysis issues, our group developed and pursued since 2003 an independent analysis of HARP large-angle data.

In this Status Report we summarize briefly the performance characteristics of the relevant detectors, the Time Projection Chamber (TPC) and the Resistive Plate Chambers (RPCs), and present an overview of physics results that we achieved and that we are confident to achieve within the next three months.

- The RPC calibration [1]
- The TPC calibration [2]
- The comparison of our $-8$ and $+8.9$ GeV/*c* Be data with Geant4 [3].

Further, we have submitted the following papers to CERN–PH management for approval as CERN–PH–EP preprints

- Cross sections on beryllium I [4]
- Cross sections on beryllium II [5].

## 2 DETECTOR CHARACTERISTICS AND PERFORMANCE

The HARP detector at the CERN PS took data in 2001 and 2002 with proton and pion beams with momentum from 1.5 to 15 GeV/*c*, with a set of stationary targets ranging from hydrogen to lead. The detector combined a forward spectrometer with a large-angle spectrometer. The latter comprised a cylindrical TPC around the target and an array of RPCs that surrounded the TPC. The purpose of the TPC was track reconstruction and particle identification by $\mathrm{d}E/\mathrm{d}x$. The purpose of the RPCs was to complement the particle identification by time of flight.

The salient technical characteristics of the TPC and the RPCs are stated in Table 1. The good particle identification capability stemming from $\mathrm{d}E/\mathrm{d}x$ in the TPC and from time of flight in the RPC's is demonstrated in Fig. 1.

Table 1: Technical characteristics of the HARP large-angle spectrometer

| **TPC** | **RPCs** |
|---|---|
| $\sigma(1/p_{\mathrm{T}}) \sim 0.20 - 0.25$ (GeV/*c*)$^{-1}$ | Intrinsic efficiency $\sim 98\%$ |
| $\sigma(\theta) \sim 9$ mrad | $\sigma$(TOF) $\sim 175$ ps |
| $\sigma(\mathrm{d}E/\mathrm{d}x)/\mathrm{d}E\mathrm{d}x \sim 0.16$ | |

## 3 COMPARISON OF GEANT4 HADRON GENERATORS WITH DATA

Precise cross-sections of secondary hadron production from the interactions of protons and pions with nuclei are of importance for the improvement and physics validation of hadron generation models in Monte Carlo simulation tool kits such as Geant4 [6].

We compared Geant4 predictions with data from the interactions with a 5% $\lambda_{\mathrm{abs}}$ beryllium target of $+8.9$ GeV/*c* protons and $\pi^+$'s, and of $-8.0$ GeV/*c* $\pi^-$'s. Details can be found in Ref. [3].

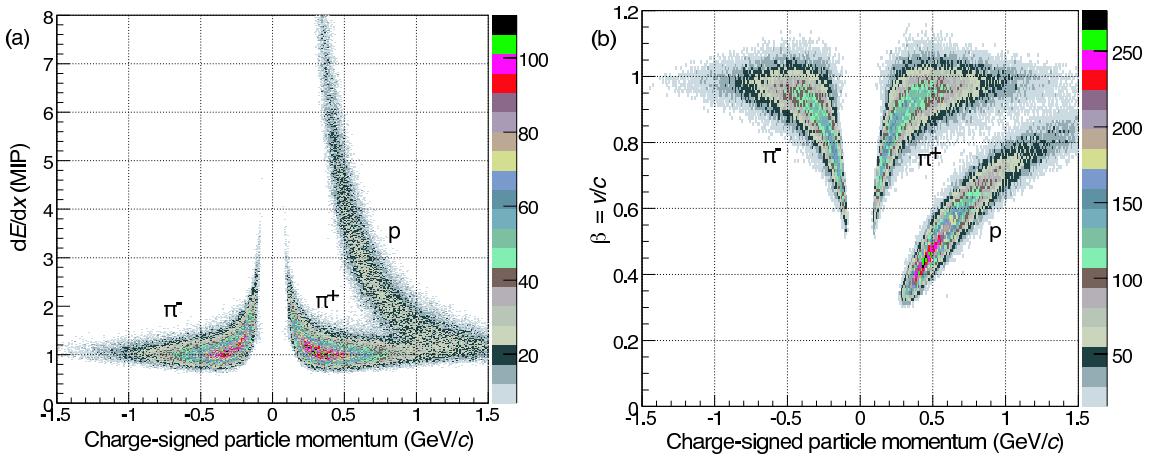


Fig. 1: Specific ionization $\mathrm{d}E/\mathrm{d}x$ (left panel) and velocity $\beta$ (right panel) versus the charge-signed momentum of positive and negative tracks in $+8.9$ GeV/$c$ data.

### 3.1 Geant4 physics lists

The Geant4 simulation tool kit provides several physics models of hadronic interactions of hadrons with nuclei, and collections of such models, termed 'physics lists'.

In the so-called 'low-energy' domain (defined as kinetic energy $E$ of the incoming hadron below $25$ GeV), a modified version of the GHEISHA package of Geant3 is used in many physics lists: the Parameterized Low-Energy Model ('LE_GHEISHA'). Optionally, for $E$ below a few GeV, the Bertini Cascade [7] ('BERT') or the Binary Cascade [8] ('BIC') models can be enabled, with a view to simulating the cascading of final-state hadrons when they move through nuclear matter. As an alternative to LE_GHEISHA, a modified version of the FRITIOF string fragmentation model [9] ('FTF') is available.

In the so-called 'high-energy' domain, mostly the Quark–Gluon String Model ('QGSM') is used, with FTF and the Parameterized High-Energy Model ('HE_GHEISHA') as alternatives. Further terms that are explained in Ref. [10], are 'PRECO' for the Pre-compound model, 'QEL' for the Quasi-elastic scattering model, and 'CHIPS' for the Chiral Invariant Phase Space model.

Figure 2 shows comparisons of polar-angle distributions of our data with three representative Geant4 physics lists: QGSP_BIC, FTFP, and QBBC. There are serious disagreements between data and model predictions.

### 3.2 HARP–CDP physics list

For the determination of hadronic cross-sections for incoming beam protons below $\sim$10 GeV/$c$ we have used the QGSP_BIC physics list. For incoming beam pions and for protons above $\sim$10 GeV/$c$, none of the standard physics lists for hadronic interactions was acceptable, so we had to build our private HARP_CDP physics list. This physics list starts from the QBBC physics list. For kinetic energy $E > 6$ GeV the Quark–Gluon String Model is replaced by the FRITIOF string fragmentation model; for $E < 6$ GeV, the Bertini Cascade is used for pion interactions, and the Binary Cascade for proton interactions; elastic and quasi-elastic scattering is disabled.

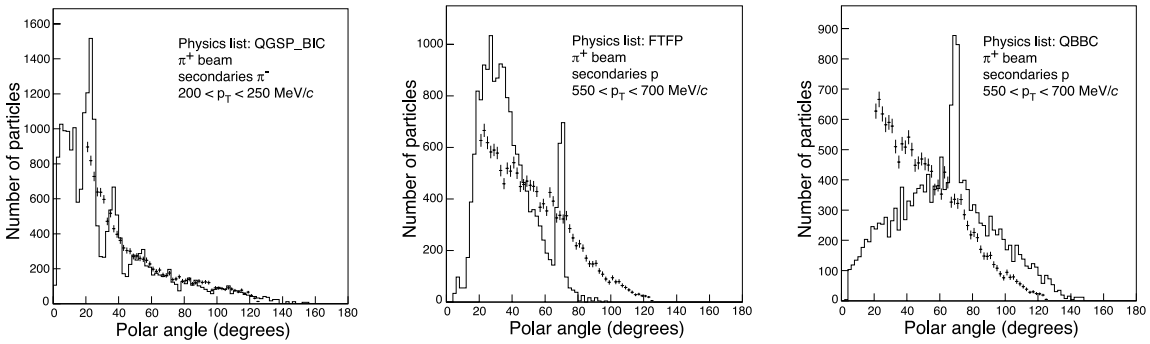


Fig. 2: QGSP_BIC physics list (left panel): polar-angle distributions of $\pi^-$'s for incoming $\pi^+$'s; FTFP physics list (middle panel): polar-angle distributions of protons for incoming $\pi^+$'s; QBBC physics list (right panel): polar-angle distributions of protons for incoming $\pi^+$'s; crosses denote data, full lines the Geant4 simulation.

Figure 3 shows the comparison of data with the simulation results from the HARP_CDP physics list. The agreement is good or at least acceptable[1)] and permits its use, after due weighting, in the analysis of the interactions of few GeV/*c* protons and pions.

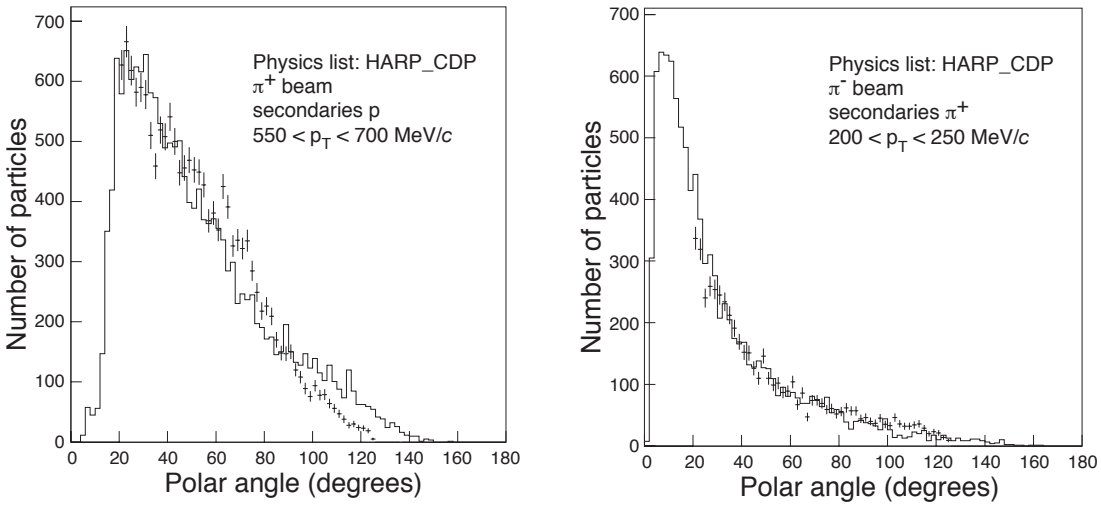


Fig. 3: HARP_CDP physics list: polar-angle distributions of protons for incoming $\pi^+$'s (left panel), and of $\pi^+$'s for incoming $\pi^-$'s (right panel); crosses denote data, full lines the Geant4 simulation.

Our observations, published in Ref. [3], led already to significant modifications in the hadron generation models by the Geant4 Collaboration.

[1)] By contrast, we define the agreement as poor if the shape of the Monte Carlo generated distribution is smooth but is grossly inconsistent with the data, or else shows structures that cannot be removed by weighting with smooth functions.

## 4 LARGE-ANGLE HADRON PRODUCTION CROSS-SECTIONS

Precise cross-sections of secondary hadron production from the interactions of protons and pions with nuclei are of importance for the understanding of the characteristics of muons from the decay of pions that are produced by the proton driver of a neutrino factory. Surprisingly, inclusive differential cross-sections of hadron production in the interactions of few GeV/*c* protons with nuclei are known only within a factor of two to three.

We have measured [4, 5] the inclusive cross-sections of the large-angle production (polar angle $\theta$ in the range from 20 to 125°) of secondary protons and charged pions in the interactions with a 5% $\lambda_{\rm abs}$ beryllium target of protons and pions with beam momenta of $\pm 3.0$, $\pm 5.0$, $-8.0$, $+8.9$, $\pm 12.0$, and $\pm 15.0$ GeV/*c*.

### 4.1 Inclusive cross-sections

Figure 4 shows examples of inclusive cross-sections of proton and $\pi^{\pm}$ production on beryllium nuclei. Double-differential cross-sections with a typical precision of a few per cent are available in tabular form in Refs. [4, 5] for the polar-angle range of 20 to 125° and for the $p_{\rm T}$ range of 0.10 to 1.25 GeV/*c*.

Figure 5 shows the inclusive cross-sections of the production of protons, $\pi^+$'s, and $\pi^-$'s, from incoming protons between 3 GeV/*c* and 15 GeV/*c* momentum, as a function of their charge-signed $p_{\rm T}$. The data refer to the polar-angle range $20^\circ < \theta < 30^\circ$. There are rather strong differences in the production of proton, $\pi^+$ and $\pi^-$ secondaries for different beam particles and beam momenta.

In Fig. 6, we present the inclusive cross-sections of the production of secondary $\pi^+$'s and $\pi^-$'s, integrated over the momentum range $0.2 < p < 1.0$ GeV/*c* and the polar-angle range $30^\circ < \theta < 90^\circ$ in the forward hemisphere, as a function of the beam momentum. We draw attention to the differences in the energy-dependence of the cross-sections for different combinations of beam particle and secondary hadron.

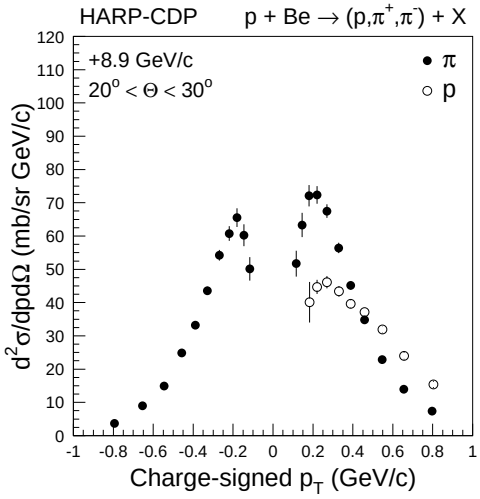


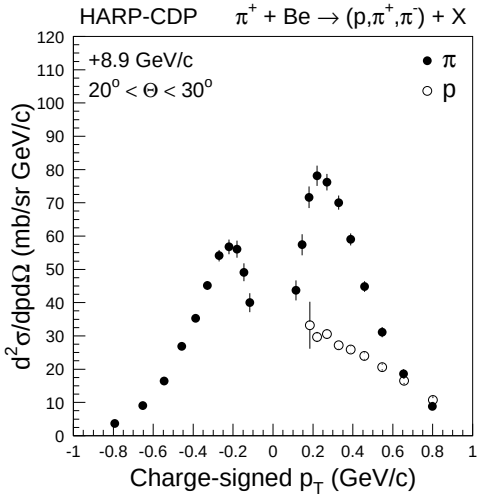


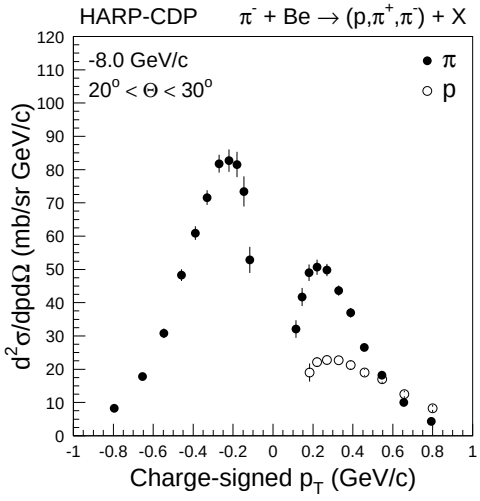


Fig. 4: Inclusive cross-sections of the production of secondary protons, $\pi^+$'s, and $\pi^-$'s, in the polar-angle range 20 to 30°, by protons (upper panel), $\pi^+$ (middle panel) and $\pi^-$ (lower panel) with beam momentum of $+8.9$ GeV/$c$ on beryllium nuclei, as a function of the charge-signed $p_{\mathrm{T}}$ of the secondaries; the shown errors are total errors.

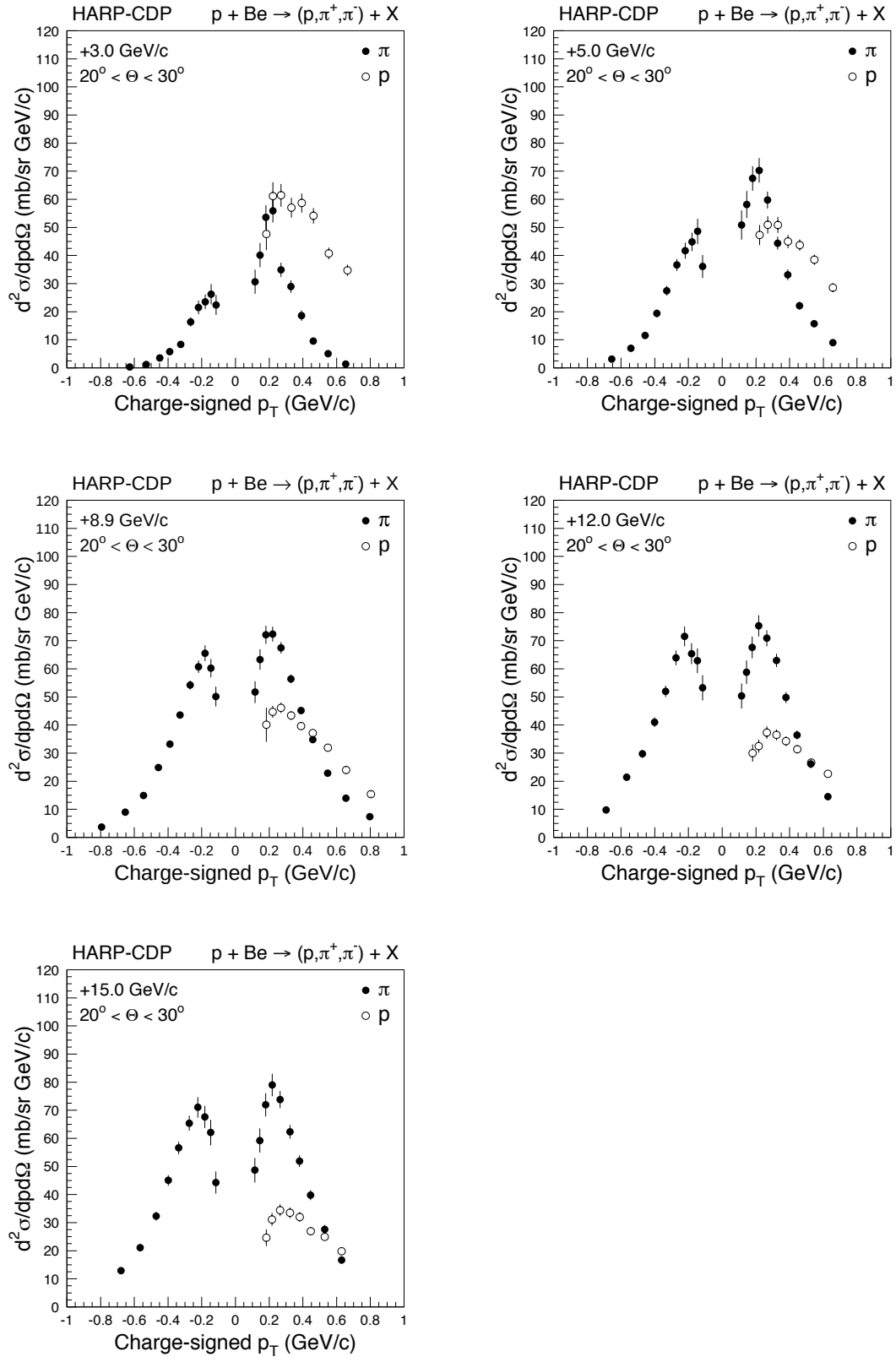


Fig. 5: Inclusive cross-sections of the production of secondary protons, $\pi^+$'s, and $\pi^-$'s, by protons on beryllium nuclei, in the polar-angle range $20^\circ < \theta < 30^\circ$, for different proton beam momenta, as a function of the charge-signed $p_{\mathrm{T}}$ of the secondaries; the shown errors are total errors.

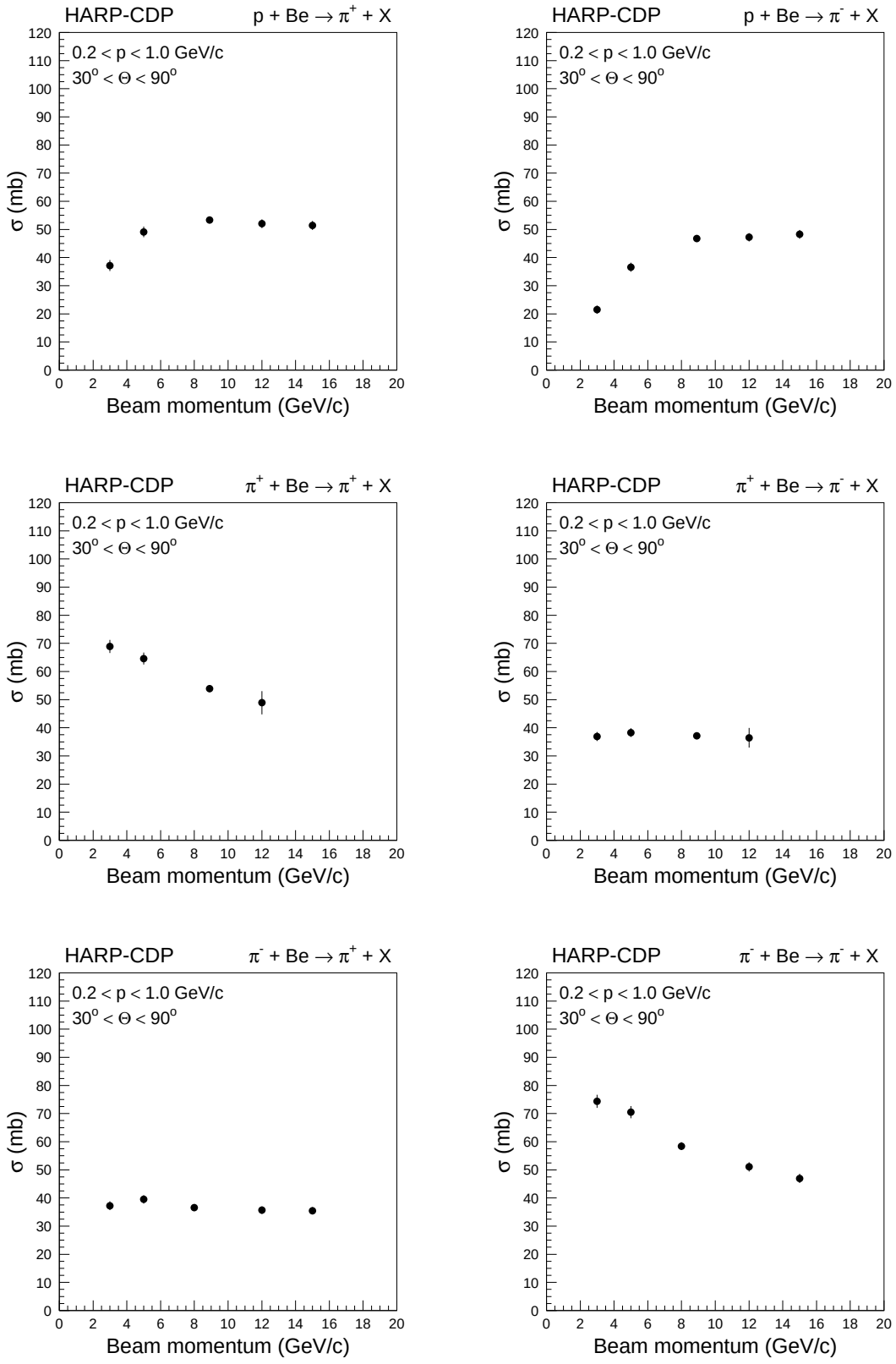


Fig. 6: Inclusive cross-sections of the production of secondary $\pi^+$'s and $\pi^-$'s, integrated over the momentum range $0.2 < p < 1.0$ GeV/$c$ and the polar-angle range $30^\circ < \theta < 90^\circ$, from the interactions on beryllium nuclei of protons (top row), $\pi^+$'s (middle row), and $\pi^-$'s (bottom row), as a function of the beam momentum; the shown errors are total errors.

### 4.2 Comparison with E802 results

Experiment E802 [11] at Brookhaven National Laboratory measured secondary $\pi^+$'s in the polar-angle range $5^\circ < \theta < 58^\circ$ from the interactions of $+14.6$ GeV/$c$ protons with beryllium nuclei.

Figure 7 shows their Lorentz-invariant cross-section of $\pi^+$ and $\pi^-$ production by $+14.6$ GeV/$c$ protons, in the rapidity range $1.2 < y < 1.4$, as a function of $m_{\rm T} - m_\pi$, where $m_{\rm T}$ denotes the pion transverse mass. Their data are compared with our cross-sections from the interactions of $+15.0$ GeV/$c$ protons with beryllium nuclei, expressed in the same unit as used by E802. Since E802 quoted only statistical errors, our data in Fig. 7 are also shown with their statistical errors.

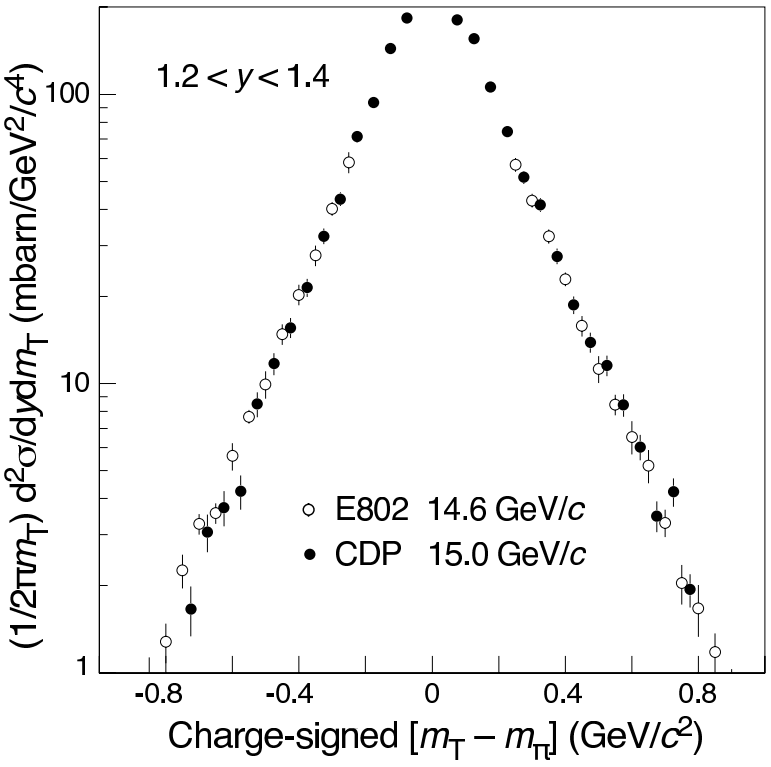


Fig. 7: Comparison of our cross-sections (black circles) of $\pi^\pm$ production by $+15.0$ GeV/$c$ protons off beryllium nuclei, with the cross-sections published by the E802 Collaboration for the proton beam momentum of $+14.6$ GeV/$c$ (open circles); all errors are statistical only.

The E802 $\pi^\pm$ cross-sections are in good agreement with our cross-sections measured nearly at the same proton beam momentum. The normalization uncertainty quoted by E802 is (10–15)%. We draw attention to the good agreement of the slopes of the cross-sections over two orders of magnitude.

### 4.3 Comparison with E910 results

Experiment E910 [12] at Brookhaven National Laboratory measured secondary charged pions in the momentum range 0.1–6 GeV/*c* from the interactions of $+12.3$ GeV/*c* protons with beryllium nuclei. This experiment used a TPC for the measurement of secondaries, with a comfortably large track length of $\sim$1.5 m. This feature, together with a magnetic field strength of 0.5 T, is of particular significance, since it permits considerably better charge identification and proton–pion separation by $\mathrm{d}E/\mathrm{d}x$ than is possible in the HARP detector. Figure 8 shows their published cross-section $\mathrm{d}^2\sigma/\mathrm{d}p\mathrm{d}\Omega$ of $\pi^{\pm}$ production by $+12.3$ GeV/*c* protons, in the polar-angle range $0.8 < \cos\theta < 0.9$. Since E910 quoted only statistical errors, our data in Fig. 8 from the interactions of $+12.0$ GeV/*c* protons are also shown with their statistical errors. The normalization uncertainty quoted by E910 is 5%.

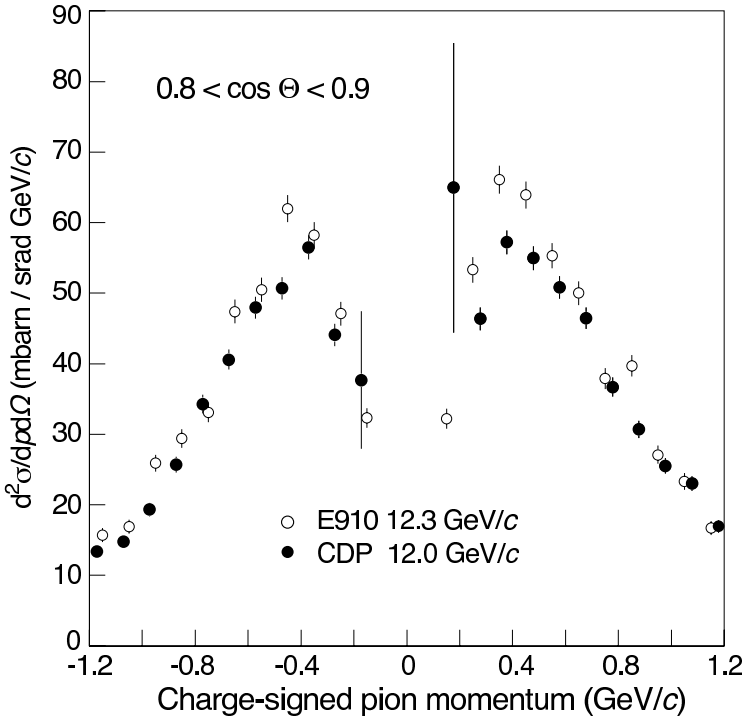


Fig. 8: Comparison of our cross-sections (black circles) of $\pi^{\pm}$ production by $+12.0$ GeV/*c* protons off beryllium nuclei with the cross-sections published by the E910 Collaboration for the proton beam momentum of $+12.3$ GeV/*c* (open circles); all errors are statistical only.

Also here, the E910 data are shown as published, and our data are expressed in the same unit as used by E910. We draw attention to the good agreement in the $\pi^+/\pi^-$ ratio between the cross-sections from E910 and our cross-sections.

### 4.4 Comparison with results from 'Official' HARP

The upper panel in Fig. 9 shows the comparison of our cross-sections of pion production by $+12.0$ GeV/*c* protons off beryllium nuclei with the ones published [13] by 'Official' HARP

(OH) in the polar-angle range $0.35 < \theta < 0.55$ rad. The latter cross-sections are plotted as published, while we expressed our cross-sections in the unit used by them. The lower panel in Fig. 9 shows our ratio $\pi^+/\pi^-$ as a function of the polar angle $\theta$ in comparison with the ratios published by the E910 Collaboration (at the slightly different proton beam momentum of $+12.3$ GeV/*c*) and by OH.

Our results are in good agreement with those of E910, however, disagree with those of OH. This discrepancy is the more striking as the same raw data were analysed by OH and by us.

The HARP Collaboration's pion production cross-sections are fatally biased. The proof of this is presented in Refs. [14, 15]. In particular, they are unsuitable for the design of a neutrino factory which was the original motivation for HARP coming into being.

### 4.5 Physics reach of HARP–CDP and of OH publications

Table 2 outlines the difference between sets of 'HARP–CDP cross-sections' and sets of 'OH cross-sections' from a given target. Other than OH, we do not restrict ourselves to

- cross-sections in the region $p < 800$ MeV/*c* (or more correctly $p_{\mathrm{T}} < 500$ MeV/*c*);
- cross-sections solely for the production of secondary pions; and
- cross-sections solely from proton beams.

Table 2: Sets of 'CDP cross-sections' vs sets of 'OH cross-sections'

| | HARP-CDP | | | OH | | |
|---|---|---|---|---|---|---|
| | Sec. p | Sec. $\pi^+$ | Sec. $\pi^-$ | Sec. p | Sec. $\pi^+$ | Sec. $\pi^-$ |
| Beam protons | yes | yes | yes | **no** | yes | yes |
| Beam $\pi^+$ | yes | yes | yes | **no** | **no** | **no** |
| Beam $\pi^-$ | yes | yes | yes | **no** | **no** | **no** |

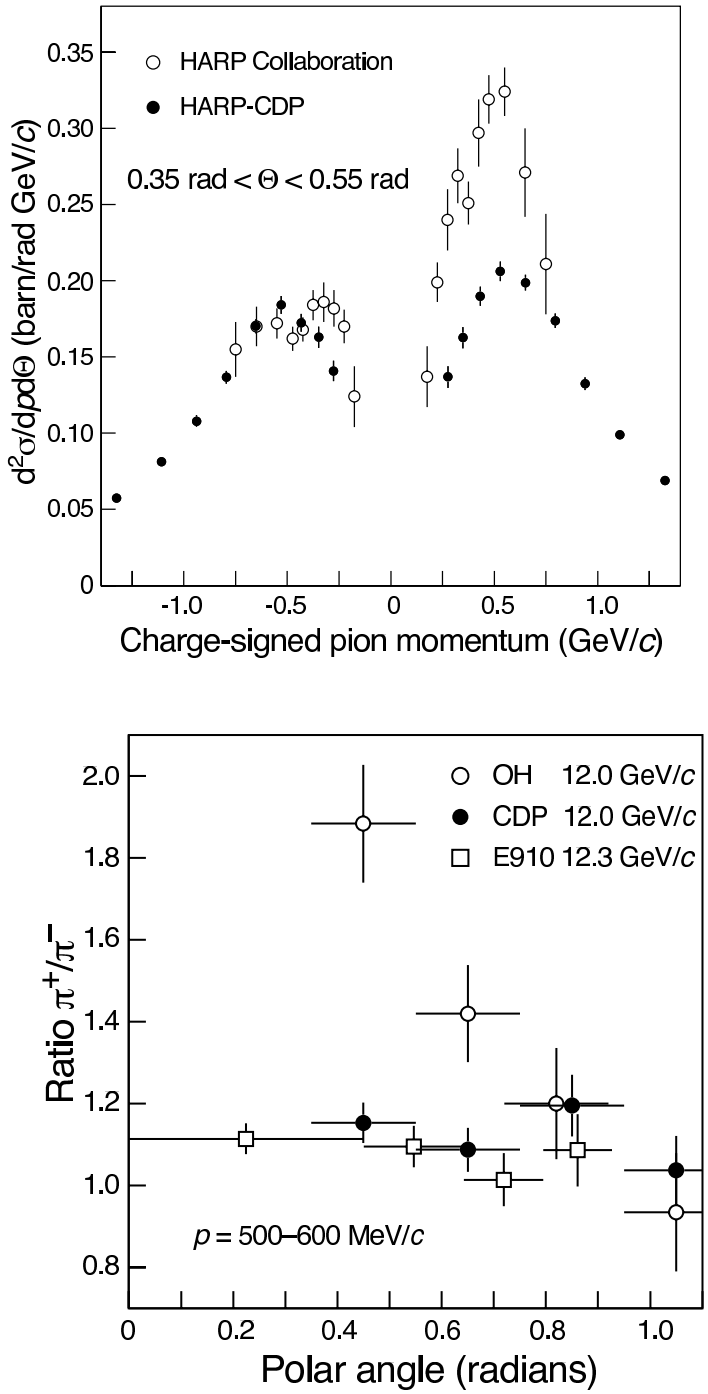


Fig. 9: Upper panel: comparison of our cross-sections (black circles) of $\pi^{\pm}$ production by $+12.0$ GeV/$c$ protons off beryllium nuclei with the cross-sections published by OH (open circles); lower panel: comparison of our ratio $\pi^{+}/\pi^{-}$ as a function of the polar angle $\theta$, with the ratios published by the E910 Collaboration and by OH; for OH, the shown errors are the total errors; for E910 and CDP, the errors are statistical only.

## 5 LSND ANOMALY

The LSND experiment at Los Alamos studied the $\bar{\nu}_e$ flux originating from protons with 800 MeV kinetic energy hitting a beam dump consisting to a good fraction of water. They reported a 3.8 $\sigma$ excess of $\bar{\nu}_e$ events over background [16]. The excess was interpreted as originating from $\bar{\nu}_\mu \rightarrow \bar{\nu}_e$ oscillation, which gave rise to many theoretical speculations as to the existence of sterile neutrinos.

The MiniBooNE Collaboration reported inconsistency of this interpretation with the findings from their search at FNAL for $\nu_\mu \rightarrow \nu_e$ oscillations [17].

A critical issue in the LSND analysis is the background level of $\bar{\nu}_e$ events that originates from the decay chain $\pi^- \rightarrow \mu^- \rightarrow \bar{\nu}_e$. An underestimate of $\pi^-$ production which was quite uncertain at the time of the LSND experiment, would reduce the anomalous excess of $\bar{\nu}_e$ events. The relevant input is a precise measurement of the ratio of secondary $\pi^-$ to $\pi^+$ production by 800 MeV protons.

With a view to clarifying this issue, the HARP detector also recorded data from the exposure of a water target to protons with 800 MeV kinetic energy (1.5 GeV/$c$ momentum).

We report peliminary ratios $\pi^-/\pi^+$ from this exposure and compare them with the ratios that were used in the LSND analysis.

Correct particle identification is of crucial importance as 800 MeV protons produce many more secondary protons than $\pi^+$'s. This is highlighted in Fig. 10 which demonstrates that the decomposition of the observed secondary particle spectrum into particle species is well understood.

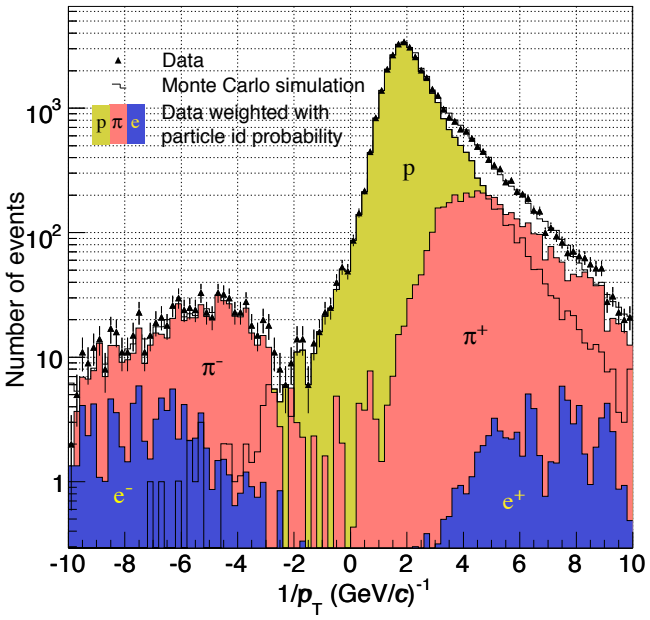


Fig. 10: Decomposition, on a logarithmic scale, of the observed spectrum of secondaries from the interaction of 800 MeV protons in water into particle species, as a function of the charge-signed $1/p_T$.

### 5.1 HARP–CDP measurements versus LSND simulations

Most positive pions from the interaction of the 800 MeV protons in the beam dump are slowed down and decay at rest, while a few per cent decay in flight. The positive muons from the decay also slow down and mostly decay at rest, with only a very small fraction decaying in flight. The neutrino flux resulting from positive pions consists of $\nu_\mu$, $\nu_\mathrm{e}$, and $\bar{\nu}_\mu$. For negative pions the decay chain is the same except for charge conjugation, yet negative pions that come to rest disappear 100% by strong interaction, and likewise negative muons at the 90% level by weak interaction. The neutrino flux resulting from negative pions can only come from pions decaying in flight, and muons decaying in orbit after capture. The neutrino flux consists of $\bar{\nu}_\mu$, $\bar{\nu}_\mathrm{e}$, and $\nu_\mu$. Overall, the $\bar{\nu}_\mathrm{e}$ which is of interest is reduced by a factor of order $10^{-4}$. In more detail, the reduction depends on the level of $\pi^-$ production, the probability of $\pi^-$ decay in flight (related to the momentum spectrum and the beam dump geometry), and of the probability of a stopped $\mu^-$ to decay in orbit.

Our measurement addresses the first of these three issues. Figure 11 shows preliminary results of the measured ratio of $\pi^-$ to $\pi^+$ production in four bins of polar angle $\theta$ with respect to the incoming proton direction. Also shown is the parametrization of this ratio that was used in the LSND analysis [18]. The measured ratio is smaller than the parametrization. Thus, if by the time of the LSND analysis our data had been known, the reported anomalous excess of $\bar{\nu}_\mathrm{e}$ events would have been even larger. Further work on this interesting result is in progress.

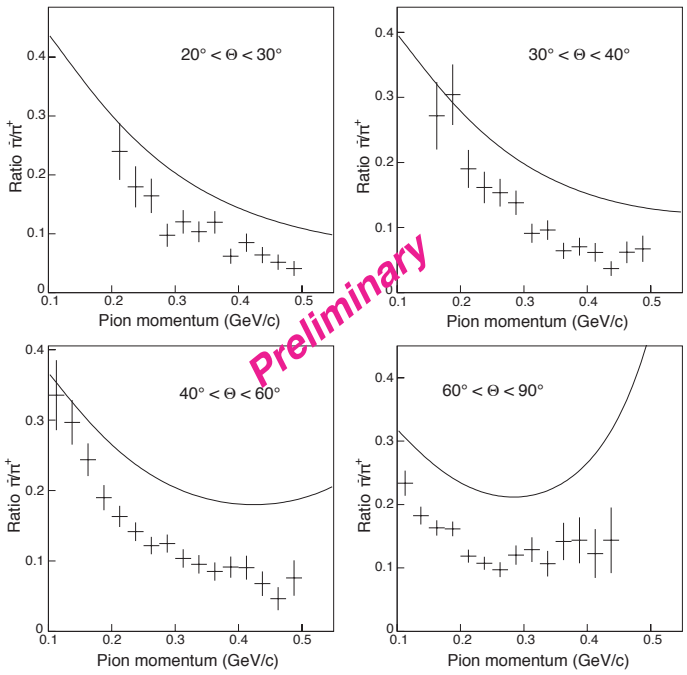


Fig. 11: Ratios $\pi^-/\pi^+$ in four bins of polar angle $\theta$ with respect to the incoming proton direction, as a function of pion momentum; the crosses denote data, the lines represent the parametrization that was used by LSND.

## 6 HARP–CDP PUBLICATIONS AND REPORTS AT CONFERENCES

Table 3 lists the number of publications, internal notes, and reports to conferences by our group, from 2003 up to now. We stress that without exception all our publications, including internal notes, were all the time publicly available on the web (http://cern.ch/harp-cdp/HARP-CDP-bibliography.pdf) and accessible for OH.

Table 3: HARP–CDP publications and reports to conferences

| | 2003 | 2004 | 2005 | 2006 | 2007 | 2008 |
|---|---|---|---|---|---|---|
| HARP memos | 3 | 6 | 3 | 6 | 3 | 2 |
| Analysis notes | | | | 2 | 3 | 1 |
| Reports to the SPSC | | 1 | 1 | | 1 | 2 |
| Publications in journals | | | | | 1 | 2 |
| Comments and Rebuttals | | | | | 2 | 3 |
| Presentations at conferences | 1 | 1 | | 1 | 1 | 3 |
| Seminars | | | | | | 3 |

## 7 PROSPECTS FOR FURTHER RESULTS FROM HARP–CDP

The commitments of HARP–CDP group members arising from the start-up of the LHC, the start of BES-III data taking, and other circumstances, mean that we have only some three to four months left for (nearly) full-time work on HARP data analysis.

The cross-sections from a thin beryllium target are completed, two physics papers have been submitted to CERN–PH for approval as CERN–PH–EP preprints.

We confirm that we will analyze rapidly and publish all cross-sections from a thin heavy target, tantalum, and from a thin target with medium atomic number, copper.

We also confirm that we will analyze rapidly and publish the $\pi^-/\pi^+$ ratio from a thick water target, including the conclusions on the LSND puzzle.

Beyond that, the situation is unclear. We consider it possible that new PhD students will continue analyzing large-angle data from thin carbon, aluminum, tin, and lead targets, if support for such activity can be found. Even if that will be possible, we anticipate that publications will emerge at a considerably slower pace.

## 8 REQUEST TO THE SPSC

In view of the unusual situation that there are two HARP groups who work independently of each other and came up with inconsistent cross-sections, and in view of the fact that the other group already published their physics results, we request the SPSC to state

1. that so far no error has been found in our analysis work, and
2. that our physics results should be published as soon as possible.

## REFERENCES


[1] V. Ammosov *et al.*, Nucl. Instrum. Methods Phys. Res. **A578** (2007) 119

[2] V. Ammosov *et al.*, Nucl. Instrum. Methods Phys. Res. **A588** (2008) 294

[3] A. Bolshakova *et al.*, Eur. Phys. J. **C56** (2008) 323

[4] A. Bolshakova *et al.*, Cross-sections of large-angle hadron production in proton– and pion–nucleus interactions I: beryllium nuclei and beam momenta of $+8.9$ GeV/*c* and $-8.0$ GeV/*c*, http://cern.ch/harp-cdp/Bepub.pdf, to be submitted to Eur. Phys. J. C.

[5] A. Bolshakova *et al.*, Cross-sections of large-angle hadron production in proton– and pion–nucleus interactions II: beryllium nuclei and beam momenta from $\pm 3$ GeV/*c* to $\pm 15$ GeV/*c*, http://cern.ch/harp-cdp/Bepub2.pdf, to be submitted to Eur. Phys. J. C.

[6] S. Agostinelli *et al.*, Nucl. Instr. and Meth. Phys. Res. **A506** (2003) 250; J. Allison *et al.*, IEEE Trans. Nucl. Sci. **53** (2006) 270

[7] M.P. Guthrie, R.G. Alsmiller and H.W. Bertini, Nucl. Instrum. Methods **66** (1968) 29

[8] G. Folger, V.N. Ivanchenko and J.P. Wellisch, Eur. Phys. J. **A21** (2004) 407

[9] B. Andersson, G. Gustafson and B. Nielsson-Almqvist, Nucl. Phys. **281** (1987) 289

[10] Geant4 Physics Reference Manual, http://geant4.web.cern.ch/geant4/UserDocumentation/UsersGuides/PhysicsReferenceManual/fo/PhysicsReferenceManual.pdf.

[11] T. Abbott *et al.*, Phys. Rev. **D45** (1992) 3906

[12] I. Chemakin *et al.*, Phys. Rev. **C65** (2002) 024904

[13] M.G. Catanesi *et al.*, Phys. Rev. **C77** (2008) 055207

[14] V. Ammosov *et al.*, Eur. Phys. J. **C54** (2008) 169

[15] V. Ammosov *et al.*, J. Instrum. **3** (2008) P01002

[16] A. Aguilar *et al.*, Phys. Rev. **D64** (2001) 112007

[17] A.A. Aguilar–Arevalo *et al.*, Phys. Rev. Lett. **98** (2007) 231801

[18] We thank Myungkee Sung for providing the LSND parametrization; the program code is available at http://hep.phys.lsu.edu/sung/lsnd/beammc/index.html